Perspectives in Cancer Research

The Glycolytic Phenotype in Carcinogenesis and Tumor Invasion: Insights through Mathematical Models

Robert A. Gatenby[1] and Edward T. Gawlinski

Departments of Radiology and Applied Mathematics, The University of Arizona, Tucson, Arizona 85724-5067 [R. A. G.], and Department of Physics, Temple University, Philadelphia, Pennsylvania 19122 [E. T. G.]

Abstract

Malignant cells characteristically exhibit altered metabolic patterns when compared with normal mammalian cells with increased reliance on anaerobic metabolism of glucose to lactic acid even in the presence of abundant oxygen. The inefficiency of the anaerobic pathway is compensated by increased glucose flux, a phenomenon first noted by Otto Warburg ~80 years ago and currently exploited for 2-fluoro-2-deoxy-D-glucose-positron emission tomography imaging in clinical radiology. The latter has demonstrated the glycolytic phenotype is a near-universal phenomenon in human cancers. The potential role of the glycolytic phenotype in facilitating tumor invasion has been investigated through mathematical models of the tumor-host interface. Modified cellular automaton and diffusion reaction models demonstrate protons will diffuse from the tumor into peritumoral normal tissue subjecting nontransformed cells adjacent to the tumor edge to an extracellular *pH* significantly lower than normal. This leads to normal cell death via *p53*-dependent apoptosis pathways, as well as degradation of the interstitial matrix, loss of intercellular gap junctions, enhanced angiogenesis, and inhibition of the host immune response to tumor antigens. Transformed cells maintain their proliferative capacity in acidic extracellular *pH* because of mutations in *p53* or some other component in the apoptosis pathways. This allows tumor cells to remain proliferative and migrate into the peritumoral normal tissue producing the invasive phenotype. Mathematical models of invasive cancer based on tumor-induced acidification are consistent with extant data on tumor microenvironment and results from clinical positron emission tomography imaging, including the observed correlation between tumor invasiveness and glucose utilization. Novel treatment approaches focused on perturbation of the tumor microenvironment are predicted from the mathematical models and are supported by recent clinical data demonstrating the benefits of azotemia and metabolic acidosis in survival of patients with metastatic renal cancer. The evolutionary basis for adoption of the glycolytic phenotype during carcinogenesis remains unclear because it appears to confer significant competitive disadvantages on the tumor cells due to of inefficient energy production and expenditure of resources to remove the acid byproducts. We propose that the glycolytic phenotype represents a successful adaptation to environmental selection parameters because it confers the ability to invade. That is, the glycolytic phenotype allows the cell to move from the microenvironment of a premalignant lesion to adjacent normal tissue. There it competes with normal cells that are less fit than the populations within the tumor in a microenvironment of relative substrate abundance. The consequent unrestrained proliferation allows the glycolytic phenotype to emerge simultaneous with the transition from a premalignant lesion to an invasive cancer.

Introduction

Theoretical oncology rarely uses quantitative methods to develop comprehensive integrative models as frameworks for interpretation, organization, and application of the vast data generated by rapid technological advances in molecular biology (1, 2). However, it is clear from centuries of experience in the physical sciences that the complex dynamics of systems dominated by nonlinear phenomena such as carcinogenesis cannot be determined by intuition and verbal reasoning alone. Rather, they must be computed through interdisciplinary, interactive research in which mathematical models, informed by extant data and continuously revised by new information, guide experimental design and interpretation.

The authors have developed working nonlinear, mathematical models of tumor invasion (3–7). The quantitative methods used were adapted to the underlying biology. Coupled partial differential equations were used for clinically apparent tumors containing large populations of transformed cells. Modified cellular automata were used to analyze very early tumor growth in which the small number of tumor cells requires discrete methods to follow the history of individual cells. This avenue of investigation is unusual because the conclusions stem entirely from mathematical analysis of the tumor-host interface.

Initial work applied methods from population biology to tumor invasion by treating tumor cells as an invading species in a previously stable multicellular ecological domain (3–5). From this, it became clear that tumor populations, as with any invading population in nature, must directly perturb the environment in a way that facilitates its growth while inhibiting those in the original community (*i.e.,* one population invades another by stealing its food or killing its young).

The search for tumor-induced perturbations in the tissue environment resulted in the acid-mediated tumor invasion model of tumor invasion (6–8). Although this approach has been extensively explored using quantitative methods (6–11), it remains obscure to the nonmathematically inclined reader. This article attempts to summarize this work in a way that is accessible to a general scientific audience.

The Acid-Mediated Tumor Invasion Model

Malignant cells are remarkably heterogeneous because of the critical role of accumulating random mutations during carcinogenesis (12, 13). The transformed genome typically exhibits hundreds, thousands, and often hundreds of thousands of genetic mutations (14), and studies of breast and renal cancers have found that every tumor cell exhibited a novel genotype (15, 16). Thus, no prototypical cancer cell genotype exists, and each invasive cancer population appears to be the result of a unique genetic pathway traveled during carcinogenesis. Yet, cancers have in common the pattern of growth characterized by progressive invasion and destruction of normal tissue leading to death of the host. This paradox of common clinical behavior despite marked genotypic diversity has been examined by the authors and collaborators (3–11). We hypothesized the similarity of invasive behavior suggests a common underlying mechanism that must be fundamen-

tally related to the few phenotypic traits exhibited by virtually all tumors. This has led us to examine in detail the potential role of altered tumor metabolism in the invasive phenotype.

Since the pioneering work of Warburg in the 1920s (17), it has been well established that tumors consistently rely on anaerobic pathways to convert glucose to ATP even in the presence of abundant oxygen. Because anaerobic metabolism of glucose to lactic acid is substantially less efficient than oxidation to CO_2 and H_2O, tumor cells maintain ATP production by increasing glucose flux. The latter forms the basis for tumor imaging with FDG-PET[2] (18–22). This technique is now widely applied to human cancers and has confirmed that the vast majority of primary and metastatic tumors demonstrate substantially increased glucose uptake compared with normal tissue. Furthermore, PET imaging has also demonstrated a direct correlation between tumor aggressiveness (and prognosis) and the rate of glucose consumption (18, 19).

A critical consequence of this altered metabolism is increased tumor cell acid production. Initially it was assumed that the lactic acid produced by anaerobic metabolism would result in an acid intracellular *pH*. However, studies with nuclear magnetic resonance spectroscopy have now consistently demonstrated that the intracellular pH of tumors is the same or slightly alkaline compared with normal cells (23) as tumor cells excrete protons through up-regulation of the Na^+/H^+ antiport and other membrane transporters. As a result, the pH_e of tumors is substantially lower (usually by ~0.5 *pH* unit) than normal (24–27).

Generally, a persistent pH_e below ~7.1 results in death of normal cells because of a *p53*-dependent apoptosis pathway triggered by increased caspase activity (28, 29). However, tumor cells are relatively resistant to acidic pH_e presumably because of mutations in *p53* or other components of the apoptotic pathway. In fact, tumor cells typically exhibit a maximum proliferation rate in relatively acidic medium (*i.e.,* pH 6.8; Refs. 30–32).

This has lead to the acid-mediated tumor invasion hypothesis (Fig. 1). The general concept is tumor cells become invasive because they perturb the environment so that it is optimal for their proliferation and toxic to the normal cells with which they compete for space and substrate (3–10). Specifically, the model proposes the following sequence:

Transformed tumor metabolism with increased glycolysis and acid excretion alters the microenvironment by substantially reducing intratumoral pH_e (25, 26). H^+ ions produced by the tumor diffuse along concentration gradients into adjacent normal tissues probably carried by a buffering species. Through a variety of mechanisms as shown in Fig. 1, acidification of the extracellular environment leads to destruction of the normal tissue. This includes normal cell death because of caspase-mediated activation of p53-dependent apoptosis pathways (28, 29), promotion of angiogenesis through acid-induced release of vascular endothelial growth factor and interleukin 8 (33), and extracellular matrix degradation by proteolytic enzymes such as cathepsin B (34) and inhibition or immune function (35). Tumor cells have an optimal pH_e significantly lower than that of normal cells (31, 32), perhaps because of mutations in *p53* or a downstream effector and so remain actively mitotic in relatively acidic pH_e. Thus, the tumor edge can be envisioned as a traveling wave extending into normal tissue after a parallel traveling wave of increased microenvironmental acidity (8).
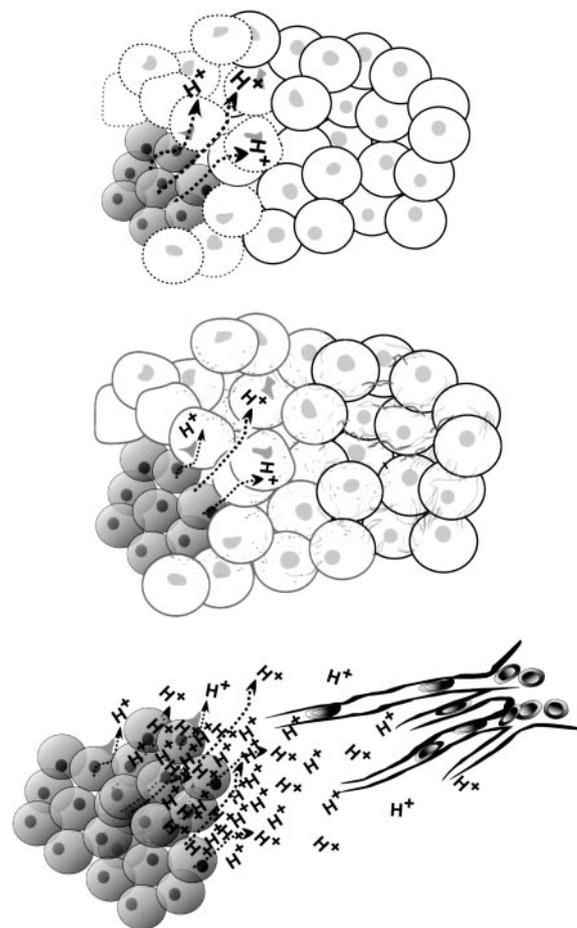
Fig. 1. Acid mediated tumor invasion. Increased acid in the tumor extracellular space because of glycolytic metabolism causes diffusion of H^+ along concentration gradients from the tumor (*dark cells*) into peritumoral normal tissues (*light cells*). The resulting decease in the pH_e causes normal cell death because of increased caspase activity, which triggers apoptosis via a p53-dependent pathway (*top picture*). In addition, the increased H^+ concentration results in extracellular matrix degradation attributable to release of cathepsin B and other proteolytic enzyme (*middle picture*) and induction of angiogenesis through release of interleukin 8 and vascular endothelial growth factor (*bottom picture*).

## Mathematical Model: Partial Differential Equations

The acid-mediated tumor invasion hypothesis can be expressed (8, 9) as a series of coupled partial differential equations that determine the spatial distribution and temporal evolution of three fields: $N_1(\mathbf{r}, t)$, the density of normal tissue (where tissue is defined as cells and their associated extracellular matrix), $N_2(\mathbf{r}, t)$, the density of tumor tissue, and $L(\mathbf{r}, t)$ the concentration of excess acid (in moles/unit volume). The differential equations governing these fields are shown in the "Appendix."

By using biologically realistic parameters based on extant data, the model predicts a gradient of excess H^+ extending from the tumor edge into adjacent normal tissue over a distance of 1–3 mm. The presence of an acidic pH_e gradient extending into peritumoral normal tissue has been confirmed using fluorescent *pH*-sensitive probes in a window chamber tumor preparation (Fig. 2). Quantitatively, the gradients are well fitted by the predictions of the model (25, 26).

Four fixed points of temporal invariance and spatial homogeneity are found in the model. One is the trivial solution: $N_1 = N_2 = 0$. In two fixed points, N_1 or N_2 achieves maximum density (*i.e.,* K_1 or K_2) while the other population vanishes. These are interpreted as resolution of the tumor with only normal tissue remaining ($N_1 = K_1$, $N_2 = 0$) and an invasive cancer ($N_1 = 0$, $N_2 = K_2$). An interesting fourth stable steady state was found in which tumor growth is highly

3848

Fig. 2. Simultaneous images of MCF7/s tumor grown in a dorsal wound chamber in a SCID mouse. The *left panel* shows a fluorescent microscopic image of the tumor, which has been transfected with green fluorescent protein and so appears lighter than the normal surrounding tissue. The *right panel* is a fluorescent ratio image with the gray scale adjusted so that darker areas have a lower pH_e. The tumor region is very acidic (*i.e.,* much darker) as compared with the (*white*) blood vessel *pH*. The pH_e in the immediate peritumoral normal tissue is somewhat less acidic but still much lower than normal, whereas the more distant normal tissue is still less acidic demonstrating the expected gradient.
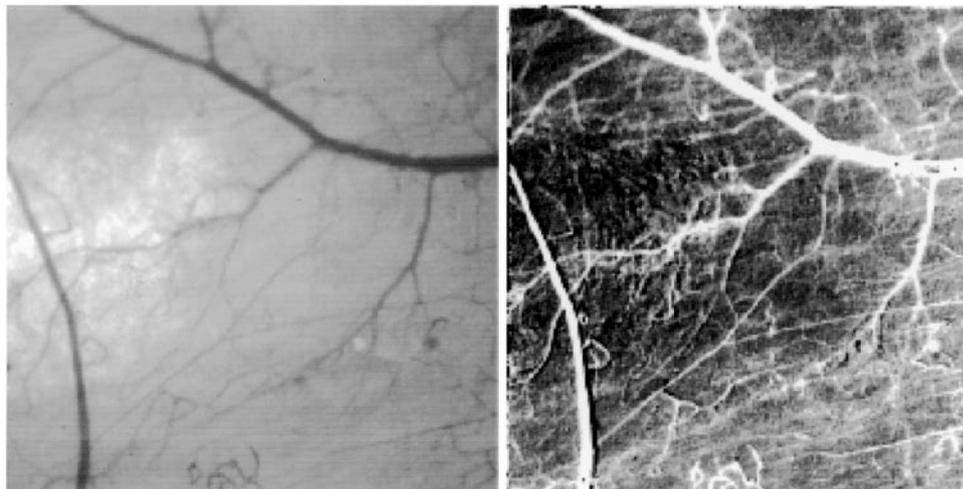
constrained and both populations persist. We interpret this state as a benign or noninvasive neoplasm. In reaction diffusion models, a stable steady state solution will invariably propagate into the unstable steady-state solution via a constant velocity traveling wave, a process that well describes the leading edge of a malignant neoplasm.

Linear stability analysis of these fixed points demonstrates that in this model normal, tissue alone ($N_1 = K_1$, $N_2 = 0$) is unconditionally unstable, whereas both the invasive cancer solution ($N_1 = 0$, $N_2 = K_2$) and the coexisting solution are conditionally but mutually exclusively stable. That is, the invasive tumor fixed point is only conditionally stable, suggesting successful tumor therapies that destabilize the tumor solution are possible. This will be further discussed below.

Depending on the value of a dimensionless parameter $\delta_1 = d_1 r_3 K_2/(d_3 r_1)$ (see "Appendix" for definitions of quantities), either the fixed point for total destruction of normal tissue ($\delta_1 > 1$) or the fourth fixed point with tumor coexisting with normal cells ($\delta_1 < 1$) is stable. Thus, although one or more of the five parameters comprising δ_1 may vary continuously with time, the entire system will change in a discontinuous, step-like manner as the value of δ_1 passes through the critical value of 1. At this point, the tumor will abruptly change from a benign pattern of growth to a malignant one (*i.e.,* with minor perturbations the system will evolve from the now unstable fourth fixed point to the stable fixed point of malignant tumor growth). Clearly, a critical parameter in this transition is the carrying capacity for the tumor population (K_2) that is presumably dependent on substrate delivery. Thus, for example, increased tumor vascularity will increase K_2 and push the system to an unstable state. This is consistent with data (36) showing that the acquisition of the angiogenic phenotype radically and abruptly alters the tumor growth from slow, noninvasive expansion in a premalignant lesion such as an adenoma to the rapid, invasive growth typical of invasive cancer. Interestingly, it appears that this analysis can be played in reverse to formulate potential tumor therapies. That is, the invasive tumor-fixed point can be rendered unstable by alterations in the critical parameters that reverse this transition. We elaborate on this point below.

The model also provides insights into the morphology of the tumor-host interface. As noted above, the tumor edge is essentially a traveling wave propagating into normal host tissue. The tumor boundary is preceded by a parallel traveling wave of excess acid produced by the transformed cells. This acidic microenvironment results in death of normal cells and the breakdown of the extracellular matrix producing available space that the tumor cells subsequently occupy. The model demonstrates that in some cases (again depending on the value of the critical parameter δ_1) the degenerating normal tissue may leave an acellular gap peripheral to the tumor boundary. We found an identifiable gap in 70% of pathologic specimens in 20 patients with squamous cell carcinoma of the head and neck (8).

Mathematical Model: Modified CA

Although tumor-induced acidification of the microenvironment may account for invasive behavior in relatively large, clinically apparent cancers, the relevance of this model to early tumor growth (such as an early metastases) was not clear. Specifically, we questioned the capacity of a few tumor cells to sufficiently alter their microenvironment to facilitate their growth at the expense of normal tissue. Modeling of this early phase of tumor growth required a new approach. Partial differential equations are well suited to modeling large cellular populations in which individual differences among the cells can be averaged. However, continuous differential equations are not applicable to small ensembles in which the activity of individual cells must be considered. CA models are optimal for this discretized approach, although traditional CA models are limited because they do not contain continuously varying elements necessary to account for diffusion reaction processes such as interstitial substrate flow and utilization.

To address these issues, we developed a modified CA model (10) as outlined in the "Appendix." The acid-mediated tumor invasion hypothesis was then evaluated by placing a small tumor nodule (5 cells in diameter for a total of 21 cells) at the center of the CA matrix initially containing normal cells and microvessels with glucose and H^+ fields at equilibrium. The models demonstrate that even a small tumor nodule will generate sufficient changes in the local microenvironment to degrade the normal tissue and allow tumor growth. Tumor growth is shown to be critically dependent on H^+ production by the transformed cells and the areal density of the microvessels. This is consistent with several areas of investigation including: (*a*) increased glucose utilization in invasive cancers compared with noninvasive (benign) tumors and evidence that adoption of the glycolytic phenotype coincides with transition from a premalignant polyp to invasive cancer in colorectal cancer (37); (*b*) a direct correlation between glucose uptake and tumor aggressiveness in sarcomas and head and neck cancers (18, 19); and (*c*) the coincidence of acquisition of the angiogenic phenotype (and, therefore, increased vascular density) and onset of invasive tumor behavior (36).

Tumor morphologies identical to those observed clinically are reproduced using this model and varying tumor acid production and

3849

Fig. 3. *A–D, left to right, top to bottom:* a wide variety of tumor morphologies and dynamics can be obtained by varying the tumor phenotype and its vascular environment. Four different tumors that have been growing for the same amount of time (40 generations), each starting from the same initial size, but with different parameter values (see appendix for definitions of $\dot{H}_T$, pH_T^Q pH_T^D and ϕ_v) are depicted. In both, *A* and *B*, $\phi_v = 0.18$ and $\dot{H}_T = 1.8 \times 10^{-4}$ mM/s, however, in *A* tumor, quiescence is admitted by setting $pH_T^Q = 6.4$, and in *B*, it is suppressed by setting $pH_T^Q = pH_T^D = 6.0$. Note that a growth rate enhancement has been obtained by the tumor in *B* at the expense of diffuse necrosis suffered throughout. In *C*, the vessel density and acid production rate have been lowered to $\phi_v = 0.08$ and $\dot{H}_T = 3.0 \times 10^{-5}$ mM/s, respectively, while keeping tumor quiescence suppressed ($pH_T^Q = 6.0$), resulting in necrosis confined to central cores. In *D*, the vascularity is lowered additionally to $\phi_v = 0.04$, resulting in a tumor that initially grows but soon self-poisons, surviving only in cords around blood vessels. The late-time growth rates of tumors in *A–C* are constant, whereas that of the tumor in *D* is decreasing. Presumably, the acquisition of additional blood supply by the tumor in D through neoangiogenesis would restore its aggressive growth.
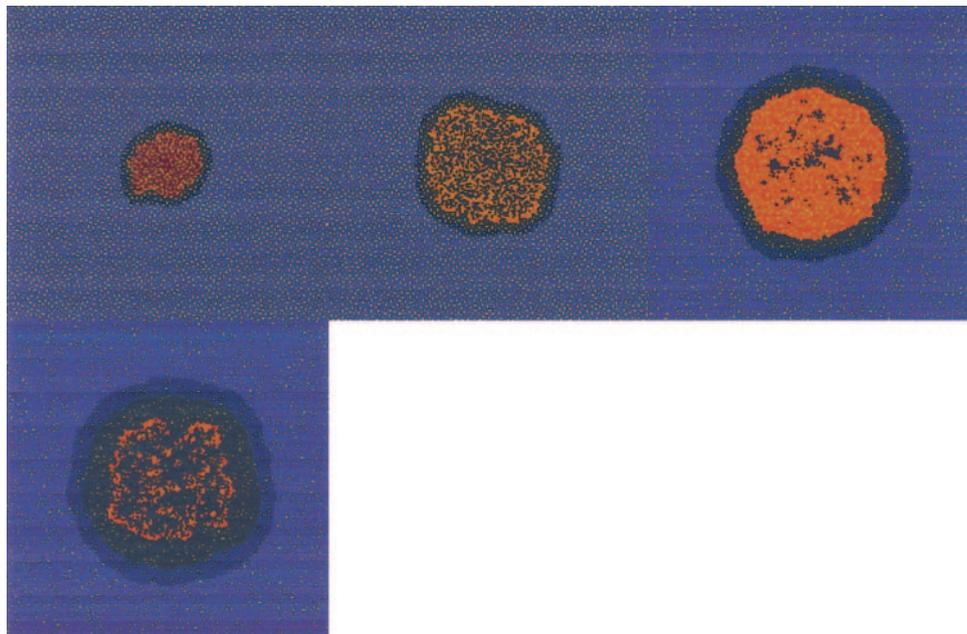
native tissue vascularity (Fig. 3). This included tumors that grew to a large volume but with a declining growth rate such that eventually (after 20 generations), no additional growth was observed, identical to the growth pattern observed in common benign tumors such as uterine leiomyoma. Highly necrotic growth with tumor cords similar to those observed in pathologic specimens of human tumors (38, 39) was demonstrated. The latter morphology is caused by a phenomenon we have termed self-poisoning. In this case, focal microenvironmental areas develop within the tumor too acidic even for transformed cells to survive. This phenomenon is dependent on the interaction of the *pH* sensitivity of the tumor cells, acid production by the tumor cells, and acid loss through the tumor vascularity. Self-poisoning will result in areas of necrosis within the tumor mass, a frequently observed pattern of growth within clinical tumors. As outlined below, therapeutic strategies designed to increase self-poisoning emerge from this model.

Implications for Treatment

Two critical observations from the mathematical models suggest novel forms of therapy. First, in the stability analysis of the diffusion reaction model, we note the critical role of δ_1 in the transition from the steady state that admits coexistence to one in which only the tumor population survives (*i.e.,* invasive cancer growth). Thus, although invasive cancer is the final result as the system evolves during carcinogenesis, the invasive tumor solution to the diffusion-reaction equations are only conditionally stable. That is, manipulation of the critical parameters that form the dimensionless parameter δ_1 could destabilize the tumor solution moving the system to another steady state. Second, the CA model demonstrates the phenomenon of self-poisoning. That is, under physiologically achievable conditions, the tumor cells may produce acid quantitatively in excess of the loss through diffusion and blood flow resulting in a microenvironment too acidic even for tumor cell growth. The resulting acid-induced tumor cell apoptosis will slow the tumor growth or even reverse tumor growth.

Thus, therapies directed toward increasing tumor acid production or decreasing acid removal through loss of tumor vascularity may decrease the propagation velocity of the tumor edge. Furthermore, manipulation of the microenvironment could destabilize the tumor solution to the state equations, resulting in cessation of tumor growth (the coexistence state) and even complete regression of the tumor (the null or normal cell only states).

In general, these results favor tumor antiangiogenesis treatment strategies because decreased vascular density will likely increase the extracellular H^+ concentrations. This will increase the probability of tumor self-poisoning and, thus, reduce the tumor growth rate. However, our results also include a cautionary note because systems with a high initial vascular density will exhibit a paradoxical increase in tumor propagation if the tumor vasculature is degraded. This phenomenon occurs because the high initial vascular density removes the excess H^+ reasonably efficiently. Perturbation of the vascular density, thus, could result in an increased peritumoral *pH* gradient, greater degradation of the normal tissue, and increased velocity of the tumor edge propagation.

It is evident from the mathematical models that therapeutic manipulation of tumor acid excretion (through drugs that inhibit the Na^+/H^+ antiport such as amiloride, for example) and vascular density are also likely to substantially reduce tumor growth rate and prolong patient survival.

One novel tumor therapy predicted by the mathematical models is manipulation of systemic *pH*. Briefly, we find that decreasing or increasing the serum acid concentration could slow tumor growth and, in some cases, even destabilize the tumor solution to the state equations (11). The latter would result in rapid evolution of the system to a new stable state: the null solution in which no remaining tumor or normal cells would remain. This would manifest clinically as an apparently spontaneous regression of the tumor.

We have recently investigated possible clinical manifestation of this mechanism (11). Several studies have demonstrated that patients with metastatic renal cancer benefit from cytoreductive nephrectomy. In rare cases (1–6% in reported series), spontaneous regression of the metastases after surgery is observed (40–42). In two recent trials, patients with metastatic renal cancer were randomized to cytoreductive nephrectomy or no surgery before systemic treatment with interleukin 2 or IFN-α (43, 44). In both studies, patients who received cytoreductive nephrectomy had statistically prolonged survival compared with the nonsurgery arm. Generally, these positive effects are
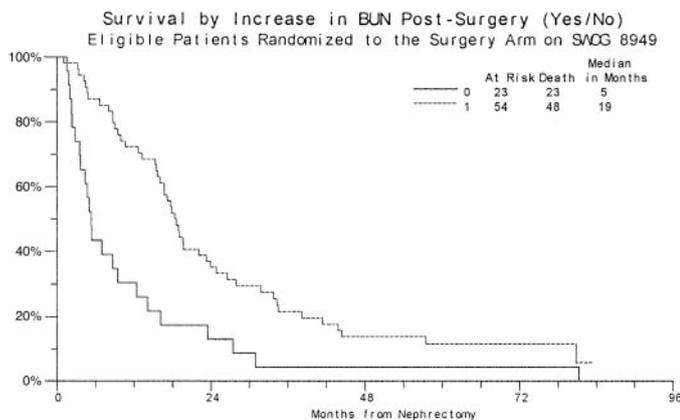
3850

Fig. 4. Survival of patients with metastatic renal cancer after cytoreductive nephrectomy with and without postoperative renal failure. As predicted by the mathematical models, postsurgical renal failure (based on elevated BUN) and the resulting mild systemic acidosis are associated with significant prolongation of survival (11).

ascribed to removal of the primary tumor because of reduction of total tumor burden, a source for positive growth factors and future metastases and enhanced immune response.

On the basis of the mathematical models, we propose an alternative hypothesis that the observed benefits are a consequence of removal of the kidney rather than the cancer. Briefly, we propose the following sequence: removal of functioning nephrons produces mild renal failure that is associated with graded metabolic acidosis. Because removal of acid from the tumor by blood vessels is dependent on the gradient of H^+ across the vessel wall, a decrease in systemic pH will reduce the vascular removal of intratumoral acid, resulting in local decrease in pH_e. If this reduction exceeds the tolerance of the tumor cells to local acidosis, the resulting cell apoptosis will decrease the tumor size and the peritumoral acid gradient, resulting in slowing and, in some cases, complete reversal of tumor growth. These changes would manifest clinically as prolonged survival for the former and apparent spontaneous regression for the latter.

This hypothesis would be supported by a correlation between postnephrectomy renal failure and subsequent length of survival. A review of the patients in the nephrectomy arm of the SWOG 8949 study has been reported (11), and the reader is referred to that publication for details of the mathematical models and the clinical data. Briefly, we found (Fig. 4) patients who developed postoperative renal failure (with an elevated BUN) had a mean survival of 19 months whereas those who did not demonstrate a change in BUN had a mean survival of 5 months ($P < 0.007$). The hypothesis is also supported by a recent study (45) of the role of acidosis in the response of melanoma xenografts to melphalan in an isolated limb perfusion study. Interestingly, in one control arm of the study, limb perfusion with media at pH 6.8 without melphalan produced 99.6% regression of the tumor because of widespread tumor cell apoptosis as predicted by the model. These results suggest that induction of brief systemic acidosis may be a viable therapeutic strategy.

Finally, the mathematical models demonstrate the potential role of the normal tissue as a barrier to tumor growth. That is, if normal cells were more resistant to tumor perturbations of the environment the ability of the tumor to invade and grow would be substantially diminished. This suggests novel therapeutic strategies directed not to the tumor but to the peritumoral normal tissues. Specifically, if normal cells could be induced to become more resistant to acid-mediated apoptosis and other effects of reduced pH_e, it appears that host resistance to tumor growth would be substantially enhanced.

The Glycolytic Phenotype in Carcinogenesis

Thus far, we have presented models of tumor invasion and not carcinogenesis. That is, the presence of malignant cells has been taken as a given. The genetic and epigenetic changes and environmental selection forces that lead to the nearly universal adoption of the glycolytic phenotype are now addressed.

The similarity of carcinogenesis to classical Darwinian evolution has often been noted. Indeed, carcinogenesis is often termed somatic evolution because it is presumably based on the dynamics of random genetic mutations and environmental selection. There is a clear association of carcinogenesis and multiple accumulating genetic mutations. Malignant cells typically contain hundreds, thousands, or even hundreds of thousands of mutations (1, 46). Detailed genetic analysis of clinical breast and renal cancers has demonstrated that every tumor has a novel pattern of genomic mutations (15, 16). The phenotypic expression of these mutants then interacts with a complex and evolving microenvironment (47, 48). Those mutations that confer a selective advantage result in clonal expansion. Because carcinogenesis appears to be dominated by these stochastic, nonlinear processes, it is not surprising that the malignant phenotype is the end point of a wide range of genetic pathways (16).

Observation of increased glycolysis in virtually all invasive cancers strongly suggests this phenotype represents a successful adaptation to some consistent environmental selection parameter.

The initial adoption of the glycolytic phenotype may well represent a response to hypoxia because of temporal and spatial heterogeneity of intratumoral blood flow. This does not, however, explain the constitutive change in metabolism that maintains high glycolytic rates even in the presence of adequate oxygen. An alternative explanation may be that the increased glucose flux imposed by adoption of the glycolytic phenotype increases expression of glucose transporters on the cell membrane and improves the cell's ability to compete for glucose in an environment in which substrate is limited. In this model, the glycolytic phenotype represents a successful adaptation in an environment in which cellular proliferation is dependent on successfully competing for limited substrate. This is analogous to a theoretical model for competing bacteria developed by Pfeiffer *et al.* (49). In this work, they note the fundamental costs and benefits of aerobic- or anaerobic-metabolic strategies. The former is maximally efficient (*i.e.,* it has the greatest yield in moles of ATP/mol of glucose) but is slow because the enzyme systems quickly saturate. The latter is inefficient but is much faster. They found that in environments with limited substrate, anaerobic metabolism is favored. Translating these results to the somatic evolution of cancer suggests that anaerobic metabolism is favored as a successful adaptation to limited glucose availability.

Probably the most straightforward explanation for the adoption of the glycolytic phenotype is simply that it is adopted because it confers the ability to invade (Fig. 5). In this sequence, we propose that cells in a preneoplastic lesion may respond to transient episodes of hypoxia by switching to glycolytic metabolism. Under usual conditions, this will be self-limited because a return of normoxic conditions will restore normal aerobic metabolism or, if glycolysis persists, the resulting pH_e acidification will result in apoptosis. However, random accumulating mutations may produce constitutive changes such that the cell is resistant to pH_e-induced apoptosis (through a *p53* mutation, for example) and remains in a fixed state of glycolysis even in the presence of oxygen. This cellular population then invades into adjacent normal tissue through the acid-mediated mechanism outlined above, conferring significant proliferative advantage on this invasive population, which now competes with less fit, nontransformed cell in

3851

ical observations. These include a biphasic pattern of cancer development with transition from premalignant (noninvasive) to malignant (invasive) morphology similar to the adenoma to carcinoma and carcinoma *in situ* to invasive cancer sequences observed in a variety of human cancers. Critical parameters in this transition include the acquisition of angiogenesis and increased glucose utilization (with increased acid production), both observed in human tumors. Furthermore, typical tumor morphologies ranging from large benign tumors to necrotic cancers growing in cords along vessels are reproduced by the models.

This hypothesis, if correct, has significant implications for cancer therapy. One possible strategy is the manipulation of the tumor-host microenvironment to foster the development of tumor necrosis through self-poisoning. This could be accomplished by either (*a*) therapies directed against tumor angiogenesis (perhaps in combination with drugs that alter the tumor cell's ability to transport H^+ across its membrane) or (*b*) therapies directed at increasing the acid concentration in the tumor by decreasing systemic *pH*. Also implicit in the models is the concept of normal tissue as a potential barrier to tumor growth. Thus, therapy that enhances the tolerance of normal cells adjacent to the tumor edge to decreased pH_e could alter the fundamental parameters of the models, resulting in absent or even negative tumor growth.

Finally, the acid-mediated tumor invasion models provide a mechanism for the near universal observation of the glycolytic phenotype in invasive human cancers. We demonstrate that the glycolytic phenotype will consistently develop during the somatic evolution of carcinogenesis precisely because it confers the ability to invade. The ability of the tumor cells to migrate into normal tissue is favored because this places the mutant population in a favorable environment in which it is unconstrained by substrate limitations or competition from other transformed cellular populations (*i.e.,* in this context normal cells are less fit than their transformed counterparts). The resulting unconstrained proliferation produces an invasive cancer.
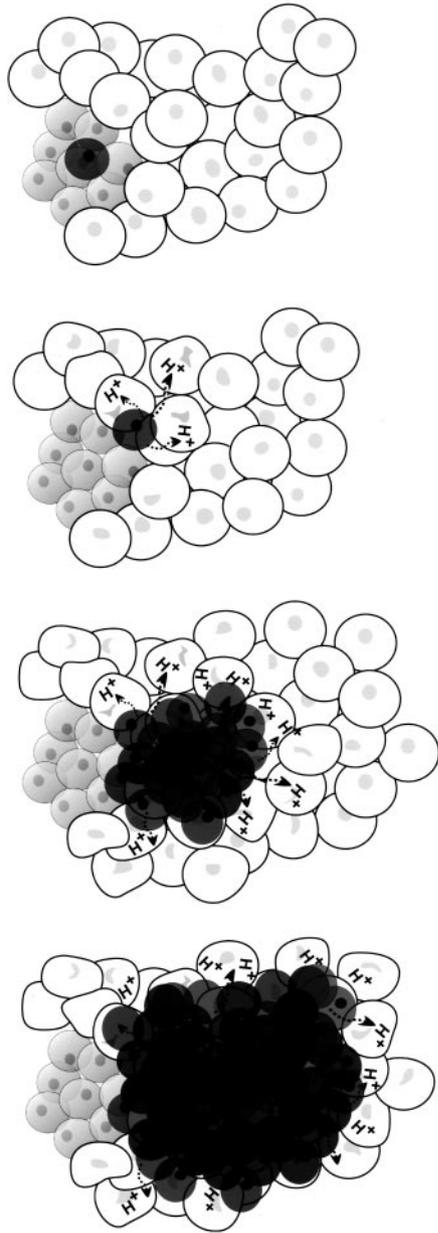

Fig. 5. Hypothesized mechanism for induction of glycolytic phenotype during carcinogenesis. Reduced vascularity and cellular crowding in preneoplastic lesions produces areas of hypoxia, requiring increased glycolytic for energy production. Through random mutations, a cell with a fixed glycolytic phenotype emerges (*top picture*). This cell or cells are able to invade into the adjacent normal tissue via mechanisms outlined in Fig. 1 (*second picture*). In the normal tissue, rapid proliferation results because of relatively abundant substrate and limited competition from the nontransformed cells (*third picture*). This produces an invasive cancer while maintaining the remnant of the original preneoplastic lesion (*bottom picture*), a phenomenon frequently observed pathologically.

an environment of substrate abundance. Clonal expansion results in persistent invasive tumor growth.

Conclusion

The acid-mediated invasion hypothesis provides a simple mechanism for malignant tumor growth that arises directly from the consistent adoption of the glycolytic phenotype with increased glucose flux and H^+ excretion almost universally observed in clinical cancers by FDG-PET imaging. Despite the underlying simplicity, the mathematical models demonstrate that acid-mediated invasion may result in highly variable and complex tumor behavior reproducing many clin-

Appendix

Partial Differential Equation Models of Tumor Invasion

The model (8) is essentially one of Lotka-Volterra interacting populations, however, it is extended to include cell death because of exposure to excess acid, acid production exclusively by tumor cells, acid reabsorption and buffering, and the spatial diffusion of acid and cells. Thus,

$$\frac{\partial N_1}{\partial t} = r_1 N_1 \left(1 - \frac{N_1}{K_1} - \alpha_{12} \frac{N_2}{K_2} \right) - d_1 L N_1 + \nabla \cdot [D_{N_1}(N_1, N_2) \nabla N_1]$$

(A1)

$$\frac{\partial N_2}{\partial t} = r_2 N_2 \left(1 - \frac{N_2}{K_2} - \alpha_{21} \frac{N_1}{K_1} \right) - d_2 L N_2 + \nabla \cdot [D_{N_2}(N_1, N_2) \nabla N_2]$$

(A2)

$$\frac{\partial L}{\partial t} = r_3 N_2 - d_3 L + D_L \nabla^2 L$$

(A3)

The parameters r_1 and r_2 are the growth rate of normal and tumor tissue, respectively, K_1 and K_2 are their carrying capacities, α_{12} and α_{21} are lumped phenomenological competition terms, which quantify the negative effects of one population on the other, and d_1 and d_2 are the cellular susceptibilities to excess acid. In the analysis discussed below, α_{12}, α_{21}, and d_2 are assumed to be small. D_{N_1} and D_{N_2} are the normal and tumor tissue diffusion or invasion coefficients. Also, $D_{N_1} = 0$ (normal tissue is well regulated) and $D_{N_2}(N_1, N_2) = D_2(1 - N_1/K_1 - N_2/K_2)$. d_3 are the combined rates of H^+ removal by

3852

blood vessels and buffering, and D_L is the diffusion coefficient for lactic acid in tissue.

Modified Cellular Automata Model

We have developed a modified cellular automata model (10) using a 200×200 matrix in which each automaton cell corresponded to either an actual physical cell having a 20-μm diameter or to a microvessel seen in cross-section.[3] Each CA element was assigned a state vector consisting of three components: (*a*) the occupancy of the space with possibilities of tumor cell, normal cell, microvessel or vacant; (*b*) interstitial glucose concentration; and (*c*) extracellular acid content. In addition, if a particular automaton cell is occupied by either a tumor or normal cell, its state vector includes a modifier indicating whether the cell is active or quiescent. This distinction will be additionally discussed below.

The microvessels are scattered randomly throughout the CA space with a concentration required to simulate a particular areal density (vessel surface area/unit volume). Vessels serve as both sources for glucose and sinks for H^+. The glucose field $G(\mathbf{r}, t)$ is governed by

$$D_G \nabla^2 G(\mathbf{r}, t) - k(\mathbf{r}, t)G(\mathbf{r}, t) = \frac{\partial G(\mathbf{r}, t)}{\partial t} \quad \text{(A4)}$$

where $\mathbf{r}$ is the position vector in the simulation space, t is time and $D_G \approx 9 \times 10^{-5}$ cm^2/s is the glucose diffusion constant. $k(\mathbf{r}, t)$ is the glucose consumption rate that is 0 for vacant cells and microvessels and equal to $k_N \approx O[10^{-4}$/s] for normal cells and $k_T \approx O[10^{-3}$/s] for tumor cells.

Glucose enters the system through boundary conditions at the vessel walls that ensure that the flux through the vessel wall is proportional to the concentration differences across it:

$$-D_G \mathbf{n} \cdot \nabla G|_{\text{wall}} = q_G(G_S - G|_{\text{wall}}) \quad \text{(A5)}$$

where $\mathbf{n}$ is the unit normal vector pointing orthogonally outward from the vessel wall, $G_S \approx 5.0$ mM is the serum glucose concentration, and $q_G \approx 3.0 \times 10^{-5}$ cm/s is the vessel permeability to glucose.

Similarly, the acid profile $H(\mathbf{r}, t)$ is described by:

$$D_H \nabla^2 H(\mathbf{r}, t) + h(\mathbf{r}, t) = \frac{\partial H(\mathbf{r}, t)}{\partial t} \quad \text{(A6)}$$

where $D_H \approx 1.1 \times 10^{-5}$ cm^2/s is the diffusion constant for lactic acid and $h(\mathbf{r}, t)$ is an acid production rate that is nonzero only at positions $\mathbf{r}$ where there are tumor cells. Acid is removed from the system again through boundary conditions at the microvessel walls:

$$-D_H \mathbf{n} \cdot \nabla H|_{\text{wall}} = q_H(H_S - H|_{\text{wall}}) \quad \text{(A7)}$$

where $q_H \approx 1.2 \times 10^{-4}$ cm/s is the vessel permeability to lactic acid, and the serum acid concentration $H_S = 3.98 \times 10^{-5}$ mM corresponds to a serum *pH* of 7.4.

A few points are in order concerning equations A4 and A6. First, the glucose consumption rate in equation A4 is proportional to the glucose concentration because it is bounded from below by 0, whereas the acid production rate in equation A6 is independent of the local acid concentration. Second, glucose consumption and acid production depend not only on position $\mathbf{r}$ but also on time t, reflecting the evolution of the system (*e.g.*, at time t an automaton cell at $\mathbf{r}$ might be occupied by a normal cell not producing acid, whereas at $t + \Delta t$ it might be occupied by an acid-producing tumor cell). Third, to better model the accumulated effects of exposure to adversely low *pH* via a discrete automaton, we have introduced the notion of active *versus* quiescent cell states. We assume there is a range of excess H^+ concentrations over which a cell is quiescent, *i.e.*, it will remain viable but will not undergo mitosis.

The rules governing the automaton are: (*a*) if the state of the automaton is either a microvessel or vacant, it does not evolve directly and (*b*) if the state of the automaton cell is either tumor or normal, the H^+ ion and glucose components of the state vector are considered. If the local *pH* is less than some

critical threshold for the normal or tumor cells (pH_N^D and pH_T^D), the cell dies and the automaton cell's state will change to vacant. In our simulations, the values $pH_N^D = 6.8$ and $pH_T^D = 6.0$ were used based on work by Dairkee *et al.* (31). If the local *pH* is greater than $pH_{N,T}^D$ but less than a second threshold $pH_{N,T}^Q$, then the cell survives in the quiescent state. The latter were taken to be $pH_N^Q = 7.1$ and $pH_T^Q = 6.4$ for normal cells and tumor cells, respectively. (*c*) If the cell is able to proliferate based on local *pH*, it will divide only if the glucose level exceeds some critical value, namely $G_{N,T}^0$. G^0 was assumed equal for tumor cells and normal cells and taken to be 2.5 mM (the serum level below which serious hypoglycemic effects are manifested).

References

1. Gatenby, R. A., and Maini, P. Modelling a new angle on understanding cancer. Nature (Lond.), *420:* 462, 2002.
2. Gatenby, R. A., and Maini, P. Mathematical oncology. Nature (Lond.), *421:* 321, 2003.
3. Gatenby, R. A. Population ecology issues in tumor growth. Cancer Res., *51:* 2542–2547, 1991.
4. Gatenby, R. A. Models of tumor-host interaction as competing populations: implications for tumor biology and treatment. J. Theor. Biol., *176:* 447–455, 1995.
5. Gatenby, R. A. Application of competition theory to tumour growth: implications for tumour biology and treatment. Eur. J. Cancer, *32A:* 722–726, 1996.
6. Gatenby, R. A. Altered glucose metabolism and the invasive tumor phenotype: insights provided through mathematical model. Int. J. Oncol., *8:* 597–601, 1996.
7. Gatenby, R. A. The potential role of transformation-induced metabolic changes in tumor-host interaction. Cancer Res., *55:* 4151–4156, 1995.
8. Gatenby, R. A., and Gawlinski, E. T. A reaction-diffusion model of acid-mediated invasion of normal tissue by neoplastic tissue. Cancer Res., *56:* 5745–5753, 1996.
9. Gatenby, R. A., and Gawlinski, E. Mathematical models of tumor invasion mediated by transformation-induced alteration of microenvironmental *pH*. In: K. A. Goode and D. J. Chadwick (eds.), The Tumour Microenvironment: Causes and Consequences of Hypoxia and acidity, pp. 85–99. Chichester, United Kingdom: John Wiley & Sons Ltd., 2001.
10. Patel, A. A., Gawlinski, E. T., Lemieux, S. K., and Gatenby, R. A. A cellular automaton model of early tumor growth and invasion: the effects of native tissue vascularity and increased anaerobic tumor metabolism. J. Theor. Biol., *213:* 315–331, 2001.
11. Gatenby, R. A., Gawlinski, E. T., Tangen, C, and Flanigan, R. C. The possible role of post operative azotemia in enhanced survival of patients with metastatic renal cancer following cytoreductive nephrectomy. Cancer Res., *62:* 5218–5222, 2002.
12. Loeb, L. A. Mutator phenotype may be required for multistage carcinogenesis. Cancer Res., *51:* 3075–3079, 1991.
13. Rabinovitch, P. S., Reid, B. J., Haggitt, R. C., Norwood, T. H., and Rubin, C. E. Progression to cancer in Barrett's esophagus is associated with genomic instability. Lab. Investig., *60:* 65–71, 1989.
14. Peinado, M. A., Malkhosyan, S., Velazquez, A., and Perucho, M. Isolation and characterization of allelic losses and gains in colorectal tumors by arbitrarily primed polymerase chain reaction. Proc. Natl. Acad. Sci. USA, *89:* 10065–10069, 1992.
15. Kerangueven, F., Noguchi, T., Coulie, R. F., Allione, F., Wargniez, V., Simony-Lafontaine, J., Longy, M., Jacquemier, J., Sobol, H., Eisinger, F., and Birnbaum, D. Genome-wide search for loss of heterozygosity shows extensive genetic diversity of human breast carcinomas. Cancer Res., *57:* 5469–5474, 1997.
16. Jiang, F., Desper, R., Papadimitriou, C. H., Schaffer, A. A., Kallioniemi, O-P., Richter, J., Schrami, P., Sauter, G., Mihatsch, M. J., and Moch, H. Construction of evolutionary tree models for renal carcinoma from comparative genomic hybridization data. Cancer Res., *60:* 6503–6509, 2000.
17. Warburg, O. The metabolism of tumors. London: Constable Press, 1930.
18. Di Chiro, G., Hatazawa, J., Katz, D. A., Rizzoli, H. V., and De Michele D. J. Glucose utilization by intracranial meningiomas as an index of tumor aggressivity and probability of recurrence: a PET study. Radiology, *64:* 521–526, 1987.
19. Haberkorn, U., Strauss, L. G., Reisser, C., Haag, D., Dimitrakopoulou, A., Ziegler, S., Oberdorfe, R. F., Rudat, V., and van Kaick, G. Glucose uptake, perfusion, and cell proliferation in head and neck tumors: relation of positron emission tomography to flow cytometry. J. Nucl. Med., *32:* 1548–1555, 1991.
20. Hawkins, R. A., Hoh, C., Glaspy, J., Choi, Y., Dahlbom, M., Rege, S., Messa, C., Nietszche, E., Hoffman, E., and Seeger, L. The role of positron emission tomography in oncology and other whole-body applications. Semin. Nucl. Med., *22:* 268–284, 1992.
21. Patz, E. F., Jr., Lowe, V. J., Hoffman, J. M., Paine, S. S., Harris, L. K., and Goodman, P. C. Persistent or recurrent bronchogenic carcinoma: detection with PET and 2-[F-18]-2-deoxy-D-glucose. Radiology, *191:* 379–382, 1994.
22. Yonekura, Y., Benua, R. S., Brill, A. B., Som, P., Yeh, S. D., Kemeny, N. E., Fowler, J. S., MacGregor, R. R., Stamm, R., Christman, D. R., and Wolf, A. P. Increased accumulation of 2-deoxy-2[^{18}F]fluoro-D-glucose in liver metastasis from colon cancer. J. Nucl. Med., *23:* 1133–1137, 1982.
23. Griffiths, J. R. Are cancer cells acidic? Br. J. Cancer, *64:* 425–427, 1991.
24. Gillies, R. J., Liu, Z., and Bhujwalla, Z. ^{31}P-MRS measurements of extracellular pH of tumors using 3-aminopropylphosphonate. Am. J. Physiol., *267:* C195–C203, 1994.
25. Martin, G. R., and Jain, R. K. Noninvasive measurement of interstitial pH profiles in normal and neoplastic tissue using fluorescent ratio imaging microscopy. Cancer Res., *54:* 5670–5674, 1994.

---

[3] A consequence of the two-dimensional nature of the automaton is translational invariance in the direction perpendicular to its plane, thus, in effect, all microvessels run parallel to this direction.

26. Martin, G. R. Thesis. In vivo pH measurement using fluorescence ratio imaging microscopy: Development and applications. Pittsburgh, PA: Carnegie Mellon University, 1995.

27. Stubbs, M., Rodriques, L., Howe, F. A., Wang, J., Jeong, K. S., Veech, R., and Griffiths, J. R. Metabolic consequences of a reversed pH gradient in rat tumors. Cancer Res., *54:* 4011–4016, 1994.

28. Park, H. J., Lyons, J. C., Ohtsubo, T., and Song, C. W. Acidic environment causes apoptosis by increasing caspase activity. Br. J. Cancer, *80:* 1892–1897, 1999.

29. Williams, A. C., Collard, T. J., and Paraskeva, C. An acidic environment leads to p53 dependent induction of apoptosis. Oncogene, *18:* 3199–3204, 1999.

30. Rubin, H. J. pH and population density in the regulation of animal cell multiplication. J. Cell Biol., *51:* 686–702, 1971.

31. Dairkee, S. H., Deng, S. H., Stampfer, M. R., Waldman, R. M., and Smith, H. S. Selective cell culture of primary breast cancer. Cancer Res., *55:* 2516–2519, 1995.

32. Casciari, J. J., Sotirchos, S. V., and Sutherland, R. M. Variations in tumor growth rates and metabolism with oxygen concentration, glucose concentration, and extracellular pH. J. Cell. Physiol., *151:* 386–394, 1992.

33. Shi, Q., Le, X., Wang, B., Abbruzzese, J. L., Xiong, Q., He, Y., and Xie, K. Regulation of vascular endothelial growth factor expression by acidosis in human cancer cells. Oncogene, *20:* 3751–3756, 2001.

34. Rohzin, J., Sameni, M., Ziegler, G., and Sloane, B. F. Pericellular pH affects distribution and secretion of cathepsin B in malignant cells. Cancer Res., *54:* 6517–6525, 1994.

35. Lardner, A. The effects of extracellular pH on immune function. J. Leukoc. Biol., *69:* 522–530, 2001.

36. Folkman, J. The role of angiogenesis in tumor growth. Semin. Cancer Biol., *3:* 65–71, 1992.

37. Yasuda, S., Fujii, H., Nakahara, Y., Nishiumi, M., Takahashi, W., Ide, M., and Shohtsu, A. 18f-FDG PET detection of colonic adenomas. J. Nucl. Med. *42:* 254–259.2001.

38. Thomlinson, R. H., and Gray, L. H. The histologic structure of some human lung cancers and the possible implications for radiotherapy. Br. J. Cancer, *9:* 537–549, 1955.

39. Holash, J., Maisonpierre, P. C., Compton, D., Boland, P., Alexander, C. R., Zagzag, D., Yancopoulos, G. D., and Wiegand, S. J. Vessel co-option, regression, and growth in tumors mediated by angiopoietins and VEGF. Science (Wash. DC), *284:* 1994–1998, 1999.

40. Montie, J. E., Stewart, B. H., Straffon, R. A. Hewitt, C. B., and Montague, D. K. The role of adjunctive nephrectomy in patients with metastatic renal cancer. J. Urol., *97:* 973–977, 1967.

41. Marcus, S. G., Choyke, P. L., Reiter, R., Jaffe, G. S., Alexander, R. B., Lineham, W. M., Rosenberg, S. A., and Walther M. M. Regression of metastatic renal cell carcinoma after cytoreductive nephrectomy. J. Urol., *150:* 463–466, 1993.

42. Gleave, M. E., Elhilali, M., Fradet, Y., Davis, I., Venner, P., Saad, F., Klotz, L. H., Moore, M. J., Paton, V., and Bajamonde, A. Interferon γ-1b compared with placebo in metastatic renal-cell carcinoma. The Canadian Urologic Oncology Group. N. Engl. J. Med., *338:* 1265–1271, 1998.

43. Mickisch, G. H., Garin, A., van Poppel, H., de Prijck, L., and Sylvester, R. Radical nephrectomy plus interferon-α-based immunotherapy compared with interferon α alone in metastatic renal-cell carcinoma. A randomized trial. Lancet, *358:* 948–949, 2001.

44. Flanigan, R. C., Salmon, S. E., Blumenstein, B. A., Bearman, S. I., McGrath, P. C., Caton, J. R., Jr., Munshi, N., and Crawford, E. D. Nephrectomy followed by interferon α-2b compared with interferon α-2b alone for metastatic renal-cell cancer. N. Engl. J. Med., *23:* 1655–1659, 2001.

45. Kelley, S. T., Manon, C., Buerk, D. G., Bauer, T. W., and Fraker, D. L. Acidosis plus melphalan induces nitric oxide-mediated tumor regression in an isolated limb perfusion human melanoma xenograft model. Surgery (St. Louis), *132:* 252–258, 2002.

46. Gray, J. W., and Collins C. Genome changes and gene expression in human solid tumors. Carcinogenesis (Lond.), *21:* 443–452, 2000.

47. Rubin, H. Selected cell and selective microenvironment in neoplastic development. Cancer Res., *61:* 799–807, 2001.

48. Park, C. C., Bissell, M. J., and Barcellos-Hoff, M. H. The influence of the microenvironment on the development of the malignant phenotype. Mol. Med. Today, *6:* 324–329, 2000.

49. Pfeiffer, T., Schuster, S., and Bonhoeffer, S. Cooperation and competition in the evolution of ATP-producing pathways. Science (Wash. DC), *292:* 504–507, 2001.

AACR American Association for Cancer Research

The Glycolytic Phenotype in Carcinogenesis and Tumor Invasion: Insights through Mathematical Models

Robert A. Gatenby and Edward T. Gawlinski

Updated version	Access the most recent version of this article at: http://cancerres.aacrjournals.org/content/63/14/3847

Cited articles	This article cites 46 articles, 18 of which you can access for free at: http://cancerres.aacrjournals.org/content/63/14/3847.full#ref-list-1
Citing articles	This article has been cited by 20 HighWire-hosted articles. Access the articles at: http://cancerres.aacrjournals.org/content/63/14/3847.full#related-urls

E-mail alerts	Sign up to receive free email-alerts related to this article or journal.
Reprints and Subscriptions	To order reprints of this article or to subscribe to the journal, contact the AACR Publications Department at pubs@aacr.org.
Permissions	To request permission to re-use all or part of this article, use this link http://cancerres.aacrjournals.org/content/63/14/3847. Click on "Request Permissions" which will take you to the Copyright Clearance Center's (CCC) Rightslink site.